스티렌-부타디엔-스티렌 블록 공중합체의 노화 거동 및 열안정성에 대한 연구

Xiong Xu, Jianying Yu[†], Canlin Zhang, Song Xu, Lihui Xue, and Dong Xie*

State Key Laboratory of Silicate Materials for Architectures, Wuhan University of Technology
*School of Materials Science and Engineering, Wuhan University of Technology
(2016년 6월 16일 접수, 2016년 7월 21일 수정, 2016년 7월 23일 채택)

Investigation of Aging Behavior and Thermal Stability of Styrene-Butadiene-Styrene Tri-block Copolymer in Blends

Xiong Xu, Jianying Yu[†], Canlin Zhang, Song Xu, Lihui Xue, and Dong Xie*

State Key Laboratory of Silicate Materials for Architectures, Wuhan University of Technology, Wuhan 430070, P.R. China
*School of Materials Science and Engineering, Wuhan University of Technology, Wuhan 430070, P.R. China
(Received June 16, 2016; Revised July 21, 2016; Accepted July 23, 2016)

Abstract: Aging behavior and thermal stability of styrene-butadiene-styrene tri-block copolymer (SBS) in blends were investigated using Fourier transform infrared spectroscopy (FTIR), X-ray photoelectron spectroscopy (XPS) and thermogravimetric analysis (TG). From the analysis of FTIR, the alcohol and carboxyl hydroxyl groups will be gradually generated during the thermal and ultraviolet aging, and the effect of short-term high temperature is more serious than long-term ultraviolet exposure on the structure of SBS; XPS results show that oxygen/carbon ratio of thermal and ultraviolet aged SBS have significantly increased, while the relative concentration of C-O-H(R) is far higher than that of COOH(R); inferred oxidation mechanism of SBS based on the analytical results of FTIR and XPS shows alcohol, carboxyl, ether, ketone, etc. have mainly formed in blends after thermal or ultraviolet aging; moreover, on account of the distribution index of carbon-oxygen binding state of thermal and ultraviolet aged SBS(respectively 3.15 and 1.28), C-O is easily produced than C=O and the effect of thermal aging is more obvious; from the results of TG, the maximum decomposition rate and temperature decrease after aging.

Keywords: styrene-butadiene-styrene tri-block copolymer (SBS), thermal aging, ultraviolet aging, oxidative degradation, blends.

Introduction

Tri-block thermoplastic copolymer poly(styrene-*b*-butadiene-*b*-styrene) (SBS) has been extensively applied in the modified asphalt materials due to the outstanding and excellent physical and mechanical performance.[1-4] Because of its structural characteristics, SBS plays a leading role in the high and low temperature performance of modified asphalt.[5-7] However, the macromolecular structure of SBS in asphalt will be continuously destroyed by the natural environment such as ultraviolet irradiation and heating or molecular oxygen.[8,9] Then, lots of road diseases such as alligator crack would have been appeared during their in-service time,[10,11] while the waste asphalt concrete from the maintenance and reconstruction becomes increasingly mounting. Hence, it is of significance to explore the possibility of high-performance recycling of SBS modified asphalt.

Rejuvenation of aged SBS modified asphalt is not only for aged asphalt, but also more for aged SBS. Some studies[12-14] have reported that aged asphalt can be recycled and reused by adding asphalt rejuvenators, but this kind of recovery is not obviously useful for the aged SBS modified asphalt because it can't recovery the molecular structure of aged SBS. To solve the rejuvenation of SBS modified asphalt, it is very important to acquire the information about the molecular structure of aged SBS. However, owing to the difficult removal of the complex chemical composition of the asphalt, it is hard to extract aged SBS from modified asphalt to analyze its structural changes.

So far, studies on direct thermal- and photo-oxidation aging of SBS have been reported in publications. For example, Xu *et al.* investigated the thermal oxidation mechanism of the tri-block copolymer SBS and pointed out that the thermal oxidation mainly caused the decreasing concentration of the unsaturated double bonds in polybutadiene (PB).[15] Moreover, Luengo *et al.* has investigated the photo-oxidative degradation mechanisms in styrene-ethylene-butadiene-styrene (SEBS) and indicated that prolonging the photo-oxidation time can degrade SEBS to form a various carbonyl-containing products.[16] Obviously, changes in molecular structure of SBS in blends, for example SBS in asphalt, after thermal- and ultraviolet- aging, are different from the neat SBS. Nevertheless, the ultraviolet- or thermal-aging of SBS in blends has rarely reported.

In this paper, high boiling point solvent dimethylbenzene was chosen to substitute for the asphalt to investigate the thermal and ultraviolet aging behavior and thermal stability of SBS in blends using FTIR, XPS and TG.

Experimental

Materials. The linear SBS (1301) was supplied by Baling Petrochemical Co., Ltd, which the average molecular weight is nearly $1.1 \times 10^4 \, \text{g·mol}^{-1}$ and the mass ratio of styrene and butadiene is 30 to 70. The dimethylbenzene (C. P.) was provided by Chinese Medicine Group Chemical Reagent Co., Ltd.

Sample Preparation. 40 g SBS was firstly dissolved in the dimethylbenzene until the homogeneous phase by slightly heating and stirring. Then, the prepared SBS solution was divided into two parts for the ultraviolet and thermal aging, among which the one for thermal aging was carried out through blowing the air (flow rate, 150~200 mL/min) into the system for 48 h at $120 \pm 5 \, ^\circ\text{C}$ while the other for ultraviolet (wavelength at 365 nm) aging was conducted for 9 d at $1500 \, \mu\text{W/cm}^2 \times 25 \pm 1 \, ^\circ\text{C}$, and meanwhile the dimethylbenzene was intermittently added into the vessel to ensure the solution concentration constant. Lastly, the aged SBS solution was transferred onto a watch-glass vessel and dried to constant weight at $40 \pm 5 \, ^\circ\text{C}$.

Fourier Transform Infrared Spectroscopy (FTIR). Investigation of the structural testing was carried out using a Nicolet 6700 FTIR spectrometer (America, high resolution was $0.019 \, \text{cm}^{-1}$) within the Mid-IR wave range between 4000 and $400 \, \text{cm}^{-1}$. Samples were tested by potassium bromide (KBr) pressed-disk method.

Changes of the functional groups were quantitatively ana-

lyzed by the relative functional group index which is calculated by the eq. (1):[17]

$$I = \frac{A_i}{A_{1600} + A_{1500} + A_{1450}} \tag{1}$$

where I refers to the characteristic functional group index; A_i refers to the absorption peak area of a certain wavenumber; $A_{1600} + A_{1500} + A_{1450}$ refers to the total peak area of benzene.

X-ray Photoelectron Spectroscopy (XPS). Structure characteristics of the samples were tested using a K-Alpha XPS (Thermo Fisher Scientific) and analyzed by the specialized software Avantage. Examined sheet samples were pretreated by the vacuum heating method, and then fixed in the sample room to be tested with an irradiation of a mono-chromatic Al Kα X-ray source (1486.6 eV). Survey spectra and C1s high resolution spectra were obtained at a certain domain.

Atomic concentration ratio can be quantitatively calculated by the following eq. (2):[18]

$$\frac{N_i}{N_j} = \frac{I_i / S_i}{I_j / S_j} \tag{2}$$

where i and j represent various elements; N is the atomic number; I is the photoelectron number per second in a specific peak area; S is the atomic sensitivity factor, in which the value of S_{C1s} and S_{O1s} is respectively 0.296 and 0.711.[18]

Thermal Analysis (TG-DTG). Thermal stability of the examined samples was investigated using a Netzsch STA 449F3 thermal analyzer (Germany) with the inert nitrogen (N_2) atmosphere and heating rate of 5 $^\circ$C/min in the temperature range of 40-800 $^\circ$C. Meanwhile, TG and DTG curves simultaneously recorded in the thermal process provided a large amount of relevant degradation information.

Results and Discussion

Qualitative Analysis of FTIR Spectra. Structural changes of SBS in different conditions are recorded and noted though middle FTIR spectra. Mid infrared spectra of the three samples is shown in Figure1 and the attribution of corresponding major characteristic groups is shown in Table 1. As is shown in Figure 1, new characteristic absorption bands at nearly 3446 and $1700 \, \text{cm}^{-1}$ obviously appear after thermal or ultraviolet aging, indicating that the oxygen-containing products such as alcohol, carboxylic acid, ester, ketone, etc. have produced and generated. Furthermore, after aging, the intensity of absorption bands at 1639 and 967, $911 \, \text{cm}^{-1}$ becomes weak and new peaks

Table 1. FTIR Major Characteristic Absorption Bands for SBS

Wavenumber (cm⁻¹)	Group/Chemical bond	Vibration type
3446	Hydroxyl	O-H stretch
1720, 1695	Carbonyl	C=O stretch
1639	Carbon-carbon double bond	C-H stretch
1181	Ether	C-O-C stretch
967, 911	Carbon-carbon double bond	C-H bend
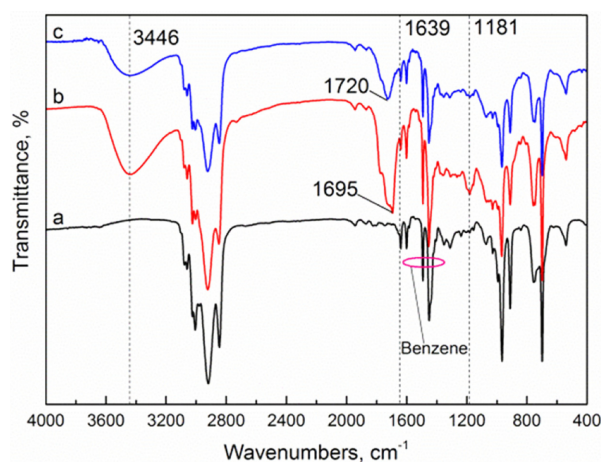
Figure 1. FTIR spectra of (a) untreated sample; (b) thermal aged sample; (c) ultraviolet aged sample.

at 1695 and 1720 cm⁻¹ appear, which implies that some of the carbon-carbon double bonds are destroyed and transform into carbonyl groups. In addition, it can be speculated that the structure of epoxy ether or fatty ether exists in the molecular chain from the new absorption peak at 1181 cm⁻¹ in the spectrum of thermal aged SBS. Regarding the formation of ether, however, it may be the random chain scission of the main chains and the epoxidation of the carbon-carbon double bonds.

Quantitative Analysis of FTIR Spectra. Table 2 presents the results of the relative functional group index obtained from FTIR spectra. It is obviously seen that the relative functional group index of carbon-carbon double bond ($I_{C=C}$) decreases and

Table 2. Results of the Relative Functional Group Index

Sample	$I_{C=C}$		$I_{C=O}$	I_{O-H}	I_{C-O-C}
	I_{1639}	I_{967}	$I_{1695\sim1720}$	I_{3446}	I_{1181}
Untreated	0.135	0.523	0	0	0.011
Thermal aged	0.043	0.289	2.024	4.053	0.314
Ultraviolet aged	0.056	0.340	1.116	2.775	0.012

that of oxygen-containing groups ($I_{C=O}$, I_{O-H}, I_{C-O-C}) increases after aging. Moreover, in this simulation environment, the residual concentration of carbon-carbon double bond after thermal aging is lower than that after ultraviolet aging, and meanwhile the concentration of the generated oxygen-containing groups after thermal aging rises higher than that after ultraviolet aging. Compared with neat SBS, I_{C-O-C} (0.314) of the thermal aged one visibly improves and that (0.012) of the ultraviolet aged one barely changes, which state SBS has a strong high temperature sensitivity in short-term aging. Besides, I_{O-H} of the thermal and ultraviolet aged SBS are respectively 4.053 and 2.775, stating that the more hydroxyl groups (-OH) have formed in thermal aging.

XPS Survey Spectra Analysis. To explain the oxidation of SBS in various environments, chemical composition changes of SBS are characterized by XPS. Figure 2 shows the XPS survey spectra of untreated, thermal and ultraviolet aged SBS. As shown in Figure 2, photoelectron and Auger electron peaks of oxygen element (O1s, O KLL) can be obviously detected in the spectra of thermal and ultraviolet aged SBS, which is correspondent with the results of FTIR. Moreover, Table 3 shows the data of the relative concentration of carbon
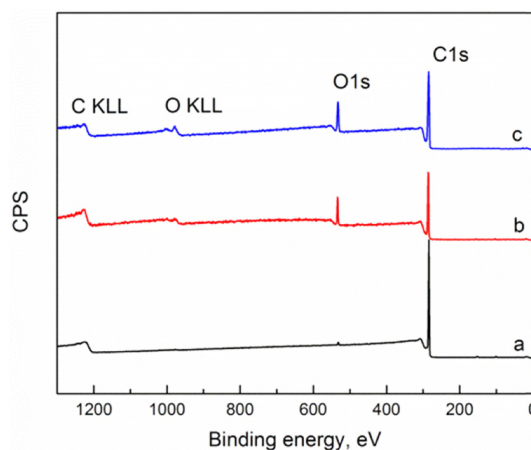
Figure 2. XPS survey spectra of (a) untreated sample; (b) thermal aged sample; (c) ultraviolet aged sample.

Table 3. Relative Concentration of Carbon and Oxygen of SBS

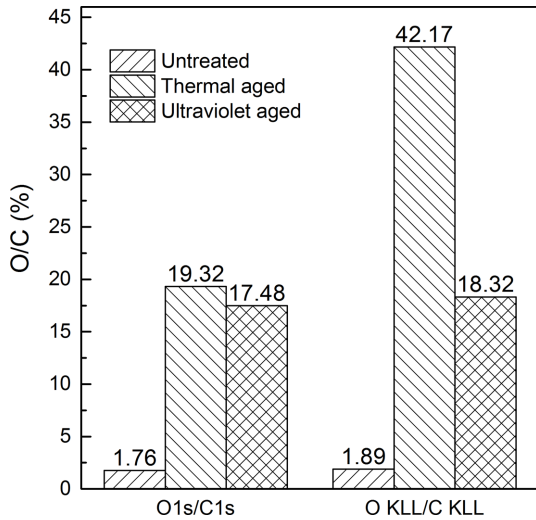| Elements	C1s (%)	O1s (%)	C KLL (%)	O KLL (%)
Untreated	92.21	1.62	5.94	0.24
Thermal aged	80.08	15.47	3.13	1.32
Ultraviolet aged	81.27	14.21	3.25	1.27

Figure 3. Oxygen/carbon ratio of SBS after exposure in different conditions.

and oxygen of SBS. Clearly, it is not difficult to find that a small amount of oxygen atoms emerge in neat SBS due to the existing antioxidant, and by comparison, after thermal aging or ultraviolet aging, the concentration of oxygen atom increases

in evidence with the decreasing concentration of carbon atom. See Figure 3, it shows the oxygen/carbon ratio of untreated, thermal aged and ultraviolet aged SBS. It can be observed that O1s/C1s and O KLL/C KLL significantly increase after aging, which implies the oxidation and degradation reaction of SBS simultaneously occurred.

XPS C1s Spectra Analysis. Chemical functional groups on SBS surface are discussed by the fitting curve of C1s spectra in Figure 4, and the relative concentrations of carbon related to chemical groups in various environments as shown in Table 4. By comparison, after exposure in the thermal or ultraviolet condition, the relative concentration of C=C (285.5 eV) obviously decreases and the oxygen-containing groups of binding energy at 286.8, 288.0, 289.0 eV attributed to C-O-H(R), C=O, COOH(R) increase, which illustrates SBS in blends still have a significant temperature and ultraviolet sensitivity and degrades into some reactive groups such as hydroxyl and carboxyl group. See Table 4, the relative concentration of C-O-H(R) of thermal aged SBS improves to a higher level than the untreated and ultraviolet aged SBS, which is in accordance with the result of FTIR.
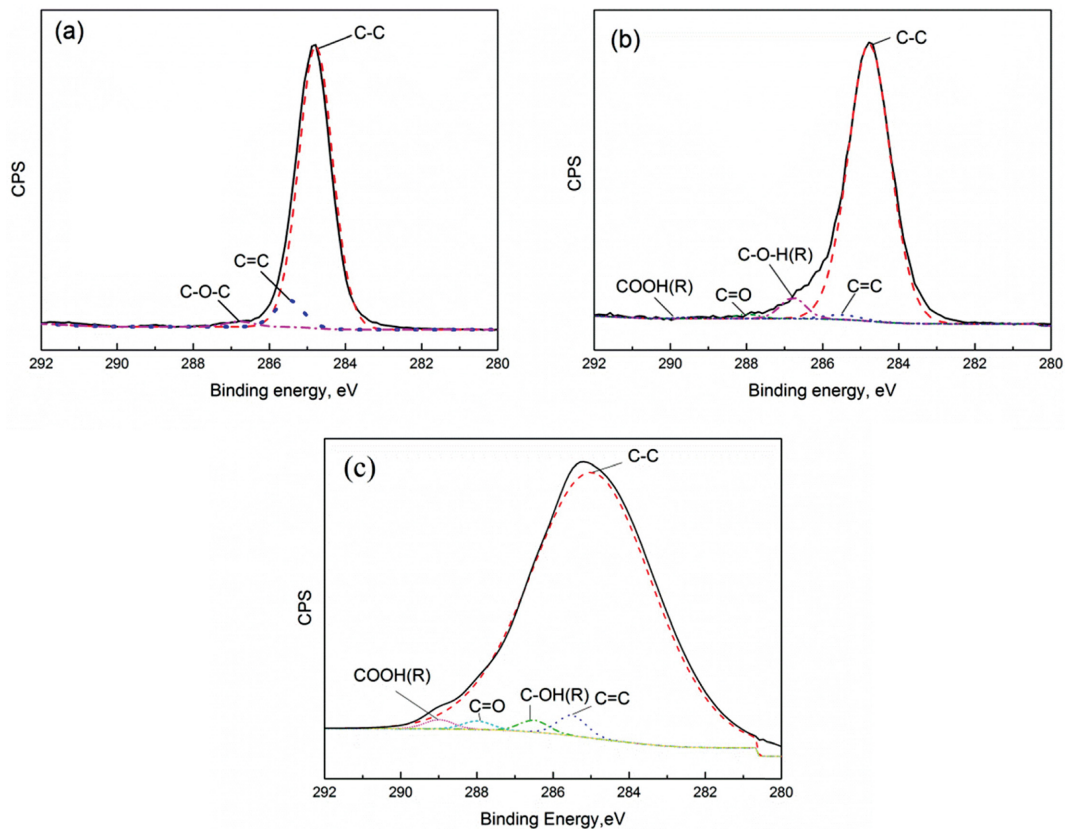

Figure 4. XPS high resolution spectra of C1s: (a) untreated sample; (b) thermal aged sample; (c) ultraviolet aged sample.

Table 4. Relative Concentrations of Carbon Related to Chemical Groups in Different Environments

Chemical state	Binding energy (eV)	Relative concentration (%)		
		Untreated	Thermal aged	Ultraviolet aged
C-C(H)	284.8±0.1	91.30	90.37	94.56
C=C	285.5±0.1	7.25	1.06	1.96
C-O-H(R)	286.8±0.1	1.45	6.44	1.59
C=O	288.0±0.1	0	1.87	1.06
COOH(R)	289.0±0.1	0	0.26	0.83

Oxidative Degradation Mechanism of α-H in SBS. Based on previous analytical results of FTIR and XPS, the oxygen-containing products, such as alcohol, carboxylic acid, carbonyl compound, ether, etc., can be obtained from whatever the thermal or ultraviolet aging. According to the reported publications,[19,20] the free radical chain reaction mechanism of the oxidative degradation of α-H in SBS can be inferred in Scheme 1. Regarding the oxidative degradation of SBS, it can be divided into four steps (initiation, propagation, transfer and termination).

At the chain initiation step, high reactive α-H atoms in PB segment are radiated and motivated into hydrogen free radicals during the exposure in heat or ultraviolet condition,[15,19,20] and then the remainders rapidly combine with molecular oxygen to form polymer peroxy radicals. Subsequently, unstable hydrogen peroxide intermediates formed by the combination of polymer peroxy radicals and hydrogen free radicals are decomposed into alkoxy and hydroxyl radicals.
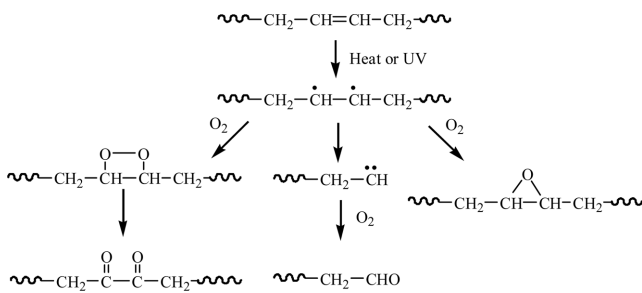
At the chain propagation step, polymer radicals continue to react with molecular oxygen for generating polymer peroxy radicals during the period of heat or ultraviolet irradiation, and afterwards the produced radicals capture α-H atoms in PB to form hydrogen peroxides and polymer radicals. Then, the chain is continuously propagating in this process.

At the chain transfer step, all kinds of stable free radicals transfer to molecular chain.

At the chain termination step, two arbitrary active free radicals interact with each other to form a stable molecule by heat and ultraviolet. Main products of the thermal and ultraviolet degradation are shown in Scheme 1(d).

Oxidative Degradation Mechanism of Carbon-carbon Double Bond in SBS. Oxidative degradation mechanism of carbon-carbon double bond in SBS is given in Scheme 2. From the scheme, π bonds in C=C of PB segments are firstly motivated to polymer radicals in the period of heat or ultraviolet,[19] while carbonyl compounds are generated by the

(a) Chain initiation

(b) Chain propagation

(c) Chain transfer

(d) Chain termination (Main products)
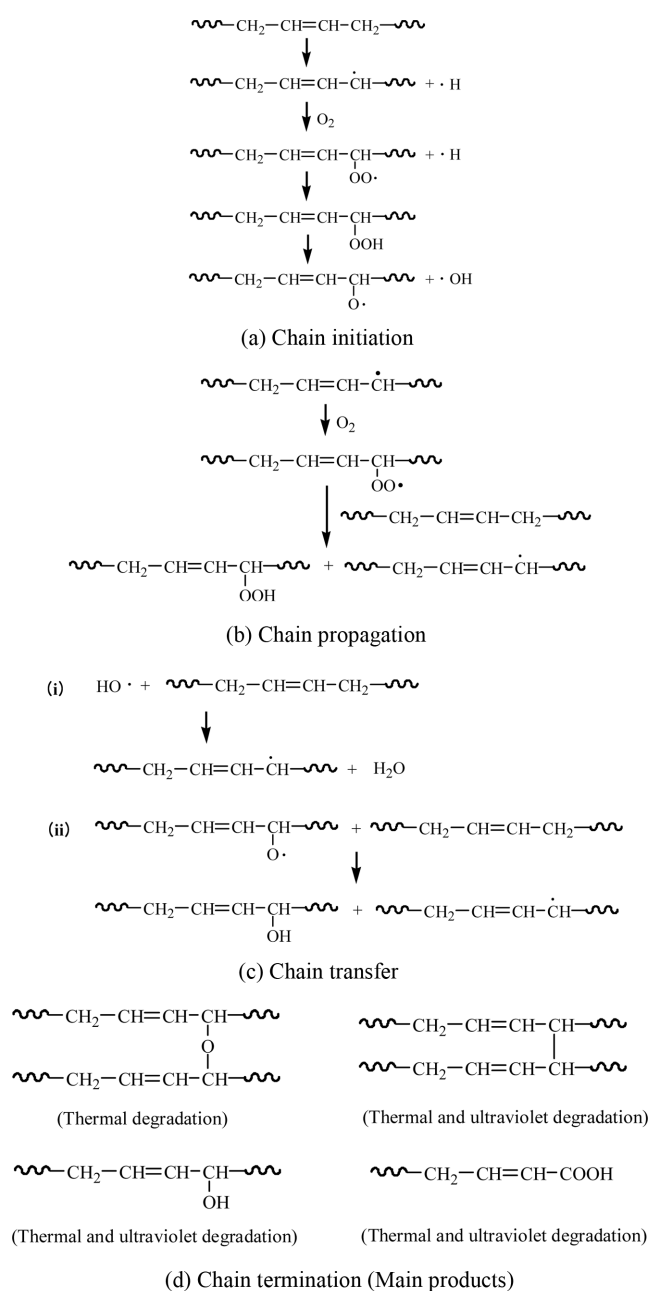
Scheme 1. Oxidative degradation mechanism of α-H in SBS.

Scheme 2. Oxidative degradation mechanism of carbon-carbon double bond in SBS.

decomposition of the unstable peroxided intermediate, epoxy ethers are obtained from the combination between polymer radicals and molecular oxygen, and aldehydes are produced by the connection of molecular oxygen and lone-pair electrons gained from the breaking C=C in PB segments.

Distribution of Carbon-oxygen Binding State. To effectively understand the distribution of carbon-oxygen single bond and double bond, the distribution index can be calculated by the following eq. (3):

$$DI = \frac{\omega_{C-O}}{\omega_{C=O}} \qquad (3)$$

where DI is the distribution index, namely the ratio of relative concentration of C-O and C=O; ω_{C-O} and $\omega_{C=O}$ are respectively the relative concentration of C-O and C=O.

On the basis of the analytic results of C1s spectra, the relative concentration of C-O and C=O and its distribution index in various environments can be summed up in Table 5. Here, distribution index is used to reflect the aging condition of SBS and judge the distribution of binding state C-O and C=O. From the oxidation mechanism above (Scheme 1 and 2), C=O may be mainly formed by the oxidation of carbon-carbon double bond and terminal hydroxyl group produced from the random chain scission, so the concentration of C=O is limited. Assuming the concentration of the formed C=O after aging is the same, the higher the value of DI, the more the concentration of

Table 5. Relative Concentration of C-O and C=O and its Distribution Index

Carbon-oxygen binding state	Relative concentration (%)		
	Untreated	Thermal aged	Ultraviolet aged
C-O	1.45	6.70	2.42
C=O	0	2.13	1.89
Distribution index	-	3.15	1.28

C-O. See Table 5, DI value of the thermal and ultraviolet aged SBS are respectively 3.15 and 1.28, which illustrates C-O is easily generated through thermal aging.

Thermal Stability. Thermal stability of neat SBS and thermal or ultraviolet aged SBS is characterized and presented in TG and DTG curves (Figures 5 and 6). Figure 5 shows the beginning decomposition temperature of SBS after exposure in thermal or ultraviolet condition shifts to the lower temperature (around 120.5 or 126.7 °C) in comparison with that of SBS (around 325.9 °C), which indicates that continuous effect of heat or ultraviolet at air atmosphere can induce the oxidative degradation of SBS. Moreover, an additional thermo-gravimetric temperature appeared in the curves of thermal aging and ultraviolet aged SBS, nearly the degradation temperature
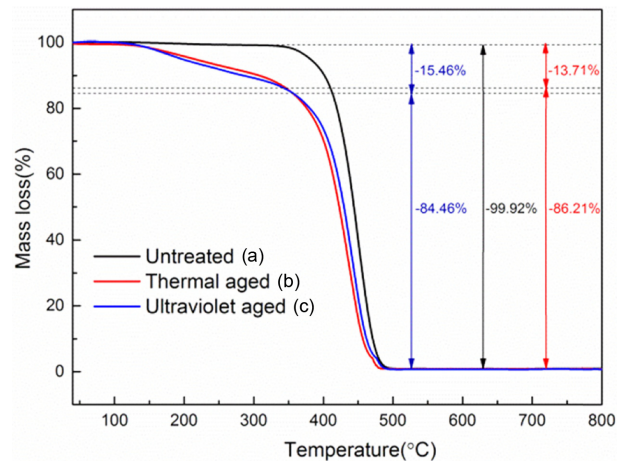

Figure 5. TG curves of (a) untreated sample; (b) thermal aged sample; (c) ultraviolet aged sample.
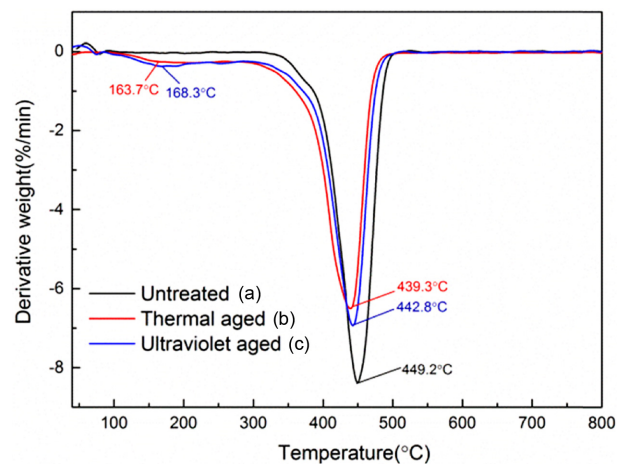

Figure 6. DTG curves of (a) untreated sample; (b) thermal aged sample; (c) ultraviolet aged sample.

of SBS, can illustrate that the initial decomposition is mainly the thermal weight loss of the degradation products (mass loss is respectively 13.71% and 15.46%) and the second weight loss is the undecomposed part of SBS (mass loss is respectively 86.21% and 84.46%). Also in Figure 6, compared with SBS, a new peak appeared at nearly 163.7 or 168.3 °C in the DTG curve of thermal or ultraviolet aged SBS identifies the existence of low molecular weight substances, namely oxidative degradation products. Meanwhile, the corresponding temperature of the maximum weight loss rate shifted to a low temperature after thermal or ultraviolet aging proves the thermal stability of SBS decreases.

Conclusions

In this work, thermal and ultraviolet ageing behavior and thermal stability of SBS in blends have been investigated. Based on the research results above, the following conclusions can be drawn. From the qualitative and quantitative analytical results of FTIR, the alcohol and carboxyl hydroxyl groups have formed during the aging, while short-term high temperature has a serious impact on the oxidative degradation of SBS than long-term ultraviolet irradiation. Results of XPS show that O/C ratio of thermal and ultraviolet aged SBS have both visibly increased, and the relative concentration of C-O-H(R) is far higher than that of COOH(R). Through the inference of oxidation mechanism based upon XPS and FTIR, the oxygen-containing groups, for instance, alcohol, carboxyl, ether, ketone, etc. have mainly formed after thermal or ultraviolet aging. Besides, distribution index of carbon-oxygen binding state of thermal and ultraviolet aged SBS are respectively 3.15 and 1.28, indicating C-O is easily generated than C=O, and the effect of thermal aging is more remarkable. TG results indicate the maximum decomposition rate and temperature both drop to a low level after aging.

References

1. C. F. Ouyang, S. F. Wang, Y. Zhang, and Y. X. Zhang, *Polym. Degrad. Stab.*, **91**, 795 (2006).
2. F. Zhang, J. Y. Yu, and S. P. Wu, *J. Hazard. Mater.*, **182**, 507 (2010).
3. B. V. Kok, M. Yilmaz, B. Sengoz, A. Sengur, and E. Avci, *Expert. Syst. Appl.*, **37**, 7775 (2010).
4. F. Q. Dong, W. Z. Zhao, Y. Z. Zhang, J. M. Wei, W. Y. Fan, and Y. J. Yu, *Constr. Build. Mater.*, **62**, 1 (2014).
5. N. L. Li, X. P. Zhao, T. H. Li, and J. Z. Pei, *Adv. Mater. Res.*, **168** 2458 (2010).
6. K. S. Hwang, W. S. Ahn, S. H. Suh, and K. R. Ha, *Polym. Korea*, **31**, 68 (2007).
7. K. S. Hwang, J. C. Lee, S. S. Jang, S. H. Lee, and K. R. Ha, *Polym. Korea*, **31**, 538 (2007).
8. M. D. Romero-Sánchez, M. M. Pastor-Blas, J. M. Martín-Martínez, and M. J. Walzak, *Int. J. Adhes. Adhes.*, **25**, 358 (2005).
9. M. S. Cortizo, D. O. Larsen, H. Bianchetto, and J. L. Alessandrini, *Polym. Degrad. Stab.*, **86**, 275 (2004).
10. F. P. Xiao, D. Newton, B. Putman, and S. N. Amirkhanian, *Mater. Struct.*, **46**, 1987 (2013).
11. F. P. Xiao, M. Chen, S. P. Wu, and S. N. Amirkhanian, *Int. J. Pavement Res. Technol.*, **6**, 496 (2013).
12. A. R. Abbas, U. A. Mannan, and S. Dessouky, *Constr. Build. Mater.*, **45**, 162 (2013).
13. M. Z. Chen, F. P. Xiao, B. Putman, B. B. Leng, and S. P. Wu, *Constr. Build. Mater.*, **59**, 10 (2014).
14. L. Sun, Y. Y. Wang, and Y. M. Zhang, *Constr. Build. Mater.*, **70**, 26 (2014).
15. J. Xu, A. Zhang, T. Zhou, X. J. Cao, and Z. N. Xie, *Polym. Degrad. Stab.*, **92**, 1682 (2007).
16. C. Luengo, N. S. Allen, M. Edge, A. Wilkinson, M. D. Parellada, and J. A. Barrio, *Polym. Degrad. Stab.*, **91**, 947 (2006).
17. W. B. Zeng, S. P. Wu, J. Wen, and Z. W. Chen, *Constr. Build. Mater.*, **93**, 1125 (2015).
18. J. F. Moulder, W. F. Stickle, P. E. Sobol, and K. D. Bomben, in *Handbook of X-ray Photoelectron Spectroscopy*, J. Chastain, Editor, Eden Prairie, MN: Perkin-Elmer, 1992.
19. B. Singh and N. Sharma, *Polym. Degrad. Stab.*, **93**, 561 (2008).
20. Y. Li, L. Li, Z. Yan, S. F. Zhao, L. D. Xie, and S. D. Yao, *J. Appl. Polym. Sci.*, **116**, 754 (2010).